Vibrational Raman Optical Activity in (*R*)-(+)-3-Methylcyclohexanone: Experimental and *ab Initio* Theoretical Studies and the Origins of the Unusual Couplets

Prasad L. Polavarapu,*,† Thomas M. Black,† Laurence D. Barron,*,‡ and Lutz Hecht‡

Contribution from the Department of Chemistry, Vanderbilt University, Nashville, Tennessee 37235, and Chemistry Department, The University, Glasgow G12 8QQ, U.K.

Received January 25, 1993

Abstract: Vibrational Raman optical activity (ROA) spectra of 3-methylcyclohexanone with excellent signal-to-noise ratio obtained on a new ROA spectrometer and corresponding *ab initio* theoretical ROA spectra obtained with 6-31G and 6-31G* basis sets are presented. The experimental ROA spectrum for the (+)-enantiomer compares well with the predicted ROA spectra for the (*R*)-configuration of 3-methylcyclohexanone. This allows us to confidently suggest the origins of several bisignate couplets present in the experimental spectrum which had previously attracted much speculative discussion.

Introduction

The potential of vibrational Raman optical activity (ROA) for three-dimensional molecular structure determination is being established rapidly. Although the ROA phenomenon was predicted[1] and observed[2] in the early 1970s, the progress in establishing ROA as a practical spectroscopic tool has been hampered by low instrumental sensitivity and lack of reliable theoretical models. Only a few years ago, the experimental measurements still appeared too difficult and successful theoretical predictions were thought to be out of reach. Recent developments both in theoretical methods and experimental techniques, however, have changed this situation. It was recognized[3,4] that ROA can be predicted from first principles, and the subsequent implementation of an *ab initio* algorithm has now made it possible to interpret experimental ROA spectra[5-13] with more confidence. At about the same time, introduction of charge coupled device (CCD) detectors into ROA spectroscopy has greatly improved the quality of ROA spectra.[14,15] It was also realized that the ROA artifacts are minimized in backscattering and that this geometry is necessary for studies on biological samples.[15,16] Different polarization modulation schemes for ROA measurements have also been formulated and implemented.[17-21] As a result of these simultaneous advances in experimental techniques and theoretical methods, ROA spectroscopy is becoming a practical tool for determining three-dimensional chiral molecular structures in the solution phase.

Methylcyclohexanone is one of the molecules that has attracted much attention for vibrational optical activity (VOA) studies in the last decade.[22-29] In the early stages of VOA research, empirical methods were tested on small molecules to verify the validity of those methods by comparing experimental observations with theoretical predictions. For theoretical predictions a knowledge of appropriate force fields with reliable force constants for the molecule under study is essential. The availability of empirical force constants for cyclohexanone[30] facilitated the situation for methylcyclohexanone because the concept of transferability of force constants appeared reasonable in these cases. Different vibrational circular dichroism (VCD)[22-24] and ROA[23,26-29] analyses were reported for 3-methylcyclohexanone. In all these studies, the vibrational assignments were derived empirically and could not be verified through an independent method. The *ab initio* quantum theoretical methods are the most reliable approaches currently available for both vibrational normal mode compositions as well as ROA predictions and therefore provide a better understanding of ROA in 3-methylcyclohexanone than the previous empirical methods. We are not aware of any prior *ab initio* vibrational studies for this molecule.

The absolute configuration and predominant conformation of (+)-3-methylcyclohexanone have been known for a long time. The (+)-enantiomer of 3-methylcyclohexanone has the (*R*)-configuration, and the chair conformation with the methyl group in an equatorial position is energetically favored over that with

† Vanderbilt University.
‡ The University, Glasgow.

(1) Barron, L. D.; Buckingham, A. D. *Mol. Phys.* **1971**, *10*, 1111.
(2) Barron, L. D.; Bogaard, M. P.; Buckingham, A. D. *J. Am. Chem. Soc.* **1973**, *95*, 603.
(3) Polavarapu, P. L. *J. Phys. Chem.* **1990**, *94*, 8106.
(4) Polavarapu, P. L. *Chem. Phys. Lett.* **1990**, *174*, 511.
(5) Bose, P. K.; Barron, L. D.; Polavarapu, P. L. *Chem. Phys. Lett.* **1989**, *155*, 423.
(6) Bose, P. K.; Polavarapu, P. L.; Barron, L. D.; Hecht, L. *J. Phys. Chem.* **1990**, *94*, 1734.
(7) Black, T. M.; Bose, P. K.; Polavarapu, P. L.; Barron, L. D.; Hecht, L. *J. Am. Chem. Soc.* **1990**, *112*, 1479.
(8) Barron, L. D.; Gargaro, A. R.; Hecht, L.; Polavarapu, P. L. *Spectrochim. Acta* **1991**, *47A*, 1001.
(9) Barron, L. D.; Gargaro, A. R.; Hecht, L.; Polavarapu, P. L. *Spectrochim. Acta* **1992**, *48A*, 261.
(10) Barron, L. D.; Gargaro, A. R.; Hecht, L.; Polavarapu, P. L.; Sugeta, H. *Spectrochim. Acta* **1992**, *48A*, 1051.
(11) Barron, L. D.; Hecht, L.; Polavarapu, P. L. *Spectrochim. Acta* **1992**, *48A*, 1193.
(12) Polavarapu, P. L.; Pickard, S. T.; Smith, H. E.; Black, T. M.; Barron, L. D.; Hecht, L. *Talanta* **1993**, *40*, 545.
(13) Polavarapu, P. L.; Hecht, L.; Barron, L. D. *J. Phys. Chem.* **1993**, *97*, 1793.
(14) Barron, L. D.; Hecht, L.; Hug, W.; MacIntosh, M. J. *J. Am. Chem. Soc.* **1989**, *111*, 8731.
(15) Barron, L. D.; Hecht, L. In *Advances in Spectroscopy*; Clark, R. J. H., Hester, R. E., Eds.; Wiley: Chichester, England, Vol. 20B, in press.
(16) Hecht, L.; Barron, L. D. *Appl. Spectrosc.* **1990**, *44*, 483.
(17) Hecht, L.; Nafie, L. A. *Mol. Phys.* **1991**, *72*, 441.
(18) Che, D.; Hecht, L.; Nafie, L. A. *Chem. Phys. Lett.* **1991**, *180*, 182.
(19) Hecht, L.; Che, D.; Nafie, L. A. *Appl. Spectrosc.* **1991**, *45*, 18.
(20) Nafie, L. A.; Freedman, T. B. *Chem. Phys. Lett.* **1989**, *154*, 260.
(21) Hecht, L.; Che, D.; Nafie, L. A. *J. Phys. Chem.* **1992**, *96*, 4266.
(22) Polavarapu, P. L.; Nafie, L. A. *J. Chem. Phys.* **1981**, *75*, 2945.
(23) Polavarapu, P. L.; Nafie, L. A. *J. Chem. Phys.* **1980**, *73*, 1567.
(24) Singh, R. D.; Keiderling, T. A. *J. Chem. Phys.* **1981**, *74*, 5347.
(25) Marcott, C.; Scanlon, K.; Overend, J.; Moscowitz, A. *J. Am. Chem. Soc.* **1981**, *103*, 483.
(26) Barron, L. D.; Clark, B. P. *J. Raman Spectrosc.* **1982**, *13*, 155.
(27) Barron, L. D.; Torrance, J. F.; Vrbancich, J. *J. Raman Spectrosc.* **1982**, *13*, 171.
(28) Freedman, T. B.; Kallmerten, J.; Zimba, C. G.; Zuk, W. M.; Nafie, L. A. *J. Am. Chem. Soc.* **1984**, *106*, 1244.
(29) Zimba, C. G.; Freedman, T. B.; Spencer, K. M.; Hu, X. M.; Nafie, L. A. *Chem. Phys. Lett.* **1987**, *134*, 233.
(30) Fuhrer, H.; Kartha, V. B.; Krueger, P. J.; Mantsch, H. H.; Jones, R. N. *Chem. Rev.* **1972**, *72*, 439.

0002-7863/93/1515-7736$04.00/0

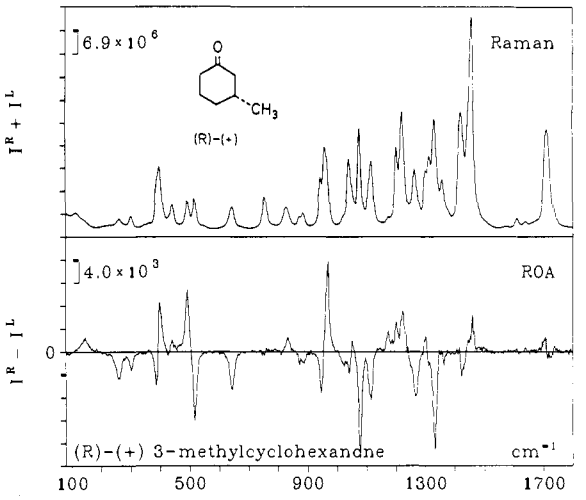

Figure 1. Experimental depolarized Raman and ROA spectra for (*R*)-(+)-3-methylcyclohexanone.

an axial methyl group and the twisted ring conformers.[31] There is no apparent need to reinvestigate the absolute configuration and conformations of methylcyclohexanone, but verifications of the ROA predictions for known structures are necessary for validating the *ab initio* theoretical model[3,4] that is in current use. Such verifications have been made for a number of small molecules including methylthiirane,[5] methyloxirane,[6,13] trans-2,3-dimethyloxirane,[7,11,13] trans-2,3-dimethylthiirane,[11,12] alanine,[8,9] tartaric acid-d_0,[10] and tartaric acid-d_4.[10] It is necessary to verify the theoretical predictions for a statistically significant number of molecules so that premature conclusions can be avoided.

In this article we report and analyze the experimental and theoretical depolarized ROA spectra for (*R*)-(+)-3-methylcyclohexanone. This study provides not only a rigorous test for the validity of the *ab initio* theoretical model currently used for ROA intensity calculations but also a detailed vibrational analysis and assignments for 3-methylcyclohexanone.

Methods

The ROA spectra were obtained on a right-angle scattering ROA spectrometer developed at Glasgow. This instrument is slightly different from the 180° backscattered ROA spectrometer reported earlier.[32] The incident Ar^+ laser beam at 488 nm with ~800-mW power at the sample was modulated between right and left circular polarization states using a KD*P electrooptic modulator at ~1/3 Hz. The 90° depolarized light wth linear polarization parallel to the scattering plane was collected and dispersed onto a backthinned, thermoelectrically cooled CCD detector (Wright Instruments). A 0.25-mm spectrograph (JY HR250S) with a 1800-grooves/mm grating was used for spectral dispersion, with a resolution of 2.4 cm^{-1} at 500 nm using the 488-nm excitation. Samples (Aldrich) were distilled twice and held in a cell (5-mm pathlength, 2 mm wide, and 10 mm high) made of fused quartz. The light scattered during left circular polarization excitation was subtracted from that during the right circular polarization excitations to give the depolarized ROA spectrum, $I^R_z - I^L_z$. The instrument calibration and sensitivity are as detailed in ref 32. The depolarized Raman and ROA spectra are shown in Figure 1. For comparison with the theoretical predictions, the normalized circular intensity difference,[1,33] $\Delta_z = (I^R_z - I^L_z)/(I^R_z + I^L_z)$ will be used.

All theoretical calculations were done with 6-31G and 6-31G* basis sets.[34] In the former basis set, the inner shell functions are expressed as linear combinations of six gaussian functions and the valence shell is split into two, one expressed with three gaussians and the second with one gaussian function. The 6-31G* basis set included, in addition, d-functions for C and O. For the ROA calculations the optical activity tensors in Cartesian displacement coordinates were evaluated with the 6-31G basis set and these tensors were converted to the normal coordinate space using the normal coordinates obtained from 6-31G as well as 6-31G* basis sets. The latter calculation involving 6-31G* normal coordinates and 6-31G Cartesian optical activity tensors is designated as 6-31G*/6-31G. The quantities involved in these calculations are given as follows:

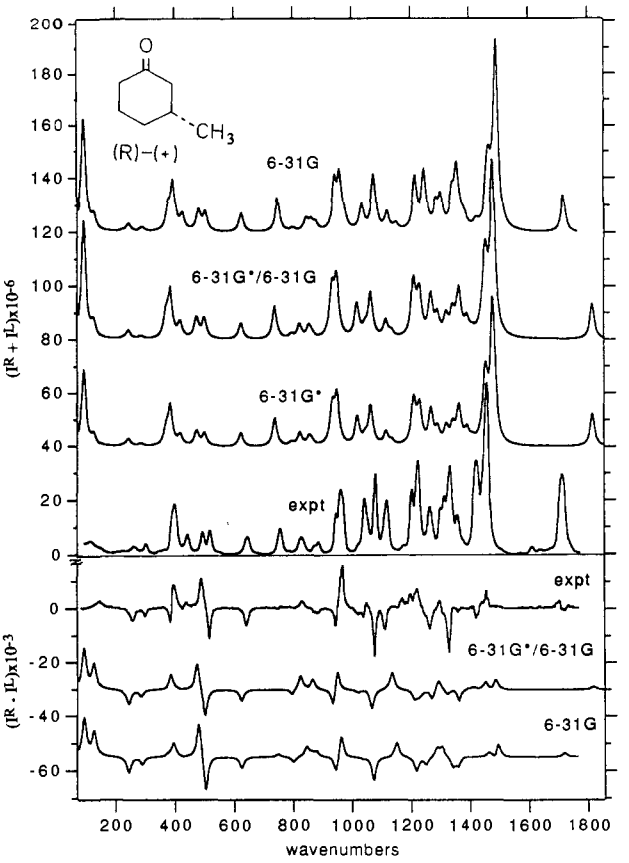

Figure 2. *Ab initio* theoretical depolarized ROA (bottom two) and Raman (top three) spectra for (*R*)-3-methylcyclohexanone. The corresponding experimental spectra for (+)-3-methylcyclohexanone are displayed in the middle (labeled expt). The theoretical spectra were simulated with Lorentzian band shapes and a 10-cm^{-1} half width after multiplying the theoretical frequencies by 0.9 to bring them closer to the experimental values. The theoretical intensities were multiplied by a constant to bring them to the same scale as that of the corresponding experimental values. The scales for $I^R + I^L$ and $I^R - I^L$ spectra differ by 10^3, and the spectra are shifted from each other for clarity in the display.

$$\Delta_z = \frac{I^R_z - I^L_z}{I^R_z + I^L_z} = \frac{24(\gamma^2 - \delta^2/3)}{12c\beta^2} \quad (1)$$

where

$$\gamma^2 = {}^1/_2\left[3\frac{\partial\alpha_{\alpha\beta}}{\partial Q}\frac{\partial G'_{\alpha\beta}}{\partial Q} - \frac{\partial\alpha_{\alpha\alpha}}{\partial Q}\frac{\partial G'_{\beta\beta}}{\partial Q}\right] \quad (2)$$

$$\delta^2 = \omega/2\frac{\partial\alpha_{\alpha\beta}}{\partial Q}\frac{\partial A_{\gamma\delta,\beta}}{\partial Q}\epsilon_{\alpha\gamma\delta} \quad (3)$$

$$\beta^2 = {}^1/_2\left[3\frac{\partial\alpha_{\alpha\beta}}{\partial Q}\frac{\partial\alpha_{\alpha\beta}}{\partial Q} - \frac{\partial\alpha_{\alpha\alpha}}{\partial Q}\frac{\partial\alpha_{\beta\beta}}{\partial Q}\right] \quad (4)$$

Here, $(\partial\alpha_{\alpha\beta}/\partial Q) = \sum_A(\partial\alpha_{\alpha\beta}/\partial X_A)(\partial X_A/\partial Q)$ with similar expressions for $(\partial G'_{\alpha\beta}/\partial Q)$ and $(\partial A_{\gamma\delta,\beta}/\partial Q)$. The $(\partial X_A/\partial Q)$ values represent atomic Cartesian displacements in a given normal mode Q and were obtained

(31) (a) Wellman, K. M.; Bunnenburg, E.; Djerassi, C. *J. Am. Chem. Soc.* **1963**, *85*, 1870. (b) Lightner, D. A.; Crist, B. V. *Appl. Spectrosc.* **1979**, *33*, 307. (c) Li, Y.-S. *J. Mol. Spectrosc.* **1987**, *122*, 490. (d) Pao, Y.; Santry, D. P. *J. Am. Chem. Soc.* **1966**, *88*, 4157. (e) Rauk, A.; Jarvie, J. O.; Ichimura, H.; Barriel, J. M. *J. Am. Chem. Soc.* **1975**, *97*, 5656. (f) Nakamura, T.; I'Haya, Y. *Bull. Chem. Soc. Jpn.* **1976**, *49*, 3461. (g) Tai, J. C.; Allinger, N. L. *J. Am. Chem. Soc.* **1966**, *88*, 2179.

(32) Hecht, L.; Barron, L. D.; Gargaro, A. R.; Wen, Z. Q.; Hug, W. *J. Raman Spectrosc.* **1992**, *23*, 401.

(33) Barron, L. D. *Molecular Light Scattering and Optical Activity*; Cambridge University Press: Cambridge, England, 1982.

(34) Hehre, W. J.; Ditchfield, R.; Pople, J. A. *J. Chem. Phys.* **1972**, *56*, 2257. Hariharan, P. C.; Pople, J. A. *Theor. Chim. Acta* **1973**, *28*, 213.

Table I. Vibrational Raman Properties of (*R*)-(+)-3-Methylcyclohexanone[a]

6-31G					6-31G*		6-31G*/6-31G			6-31G*		Experiment		Assignment[b]
mode no.	$\bar{\nu}$ (cm^{-1})	$45\bar{\alpha}^2+7\beta^2$	ρ	$\Delta_z\times10^4$	$\bar{\nu}$	scaled	$45\bar{\alpha}^2+7\beta^2$	ρ	$\Delta_z\times10^4$	$45\bar{\alpha}^2+7\beta^2$	ρ	$\bar{\nu}$	$\Delta_z\times10^4$	
13	1910	16.0	0.54	0.5	2019	1817	17.1	0.54	0.4	15.1	0.57	1710	1.7	C=O str
14	1659	13.8	0.73	1.2	1650	1485	5.9	0.73	2.8	5.1	0.71			C_β-H_2 scissor + $C_\gamma H_2$ scissor
15	1657	24.7	0.75	0.4	1644	1480	21.4	0.74	-0.2	17.8	0.74	1459	2.4	asym CH_3 bend
16	1656	18.7	0.75	0.0	1644	1480	21.6	0.75	0.1	18.1	0.75			asym CH_3 bend
17	1651	1.2	0.66	-9.4	1638	1474	4.8	0.75	-0.5	3.9	0.75			$C_\gamma H_2$ scissor + C_β-H_2 scissor
18	1633	7.9	0.74	-0.0	1620	1458	8.2	0.75	-0.3	7.0	0.74			$C_{\alpha'}$-H_2 scissor + $C_\alpha H_2$ scissor + $C_\gamma H_2$ scissor
19	1625	13.9	0.75	0.5	1613	1452	17.1	0.75	0.8	14.7	0.75	1423	-3.7	$C_\alpha H_2$ scissor + $C_{\alpha'}$-H_2 scissor
20	1580	2.0	0.73	0.2	1567	1410	1.2	0.70	3.0	1.1	0.71			sym CH_3 bend
21	1538	2.7	0.65	0.4	1547	1392	4.4	0.69	0.4	3.9	0.66	1363	-22.9	$C_\gamma H_2$ wag + $C_\beta H$ bend + C_β-C_γ str
22	1525	1.9	0.73	0.5	1519	1367	7.2	0.74	0.7	5.7	0.75			C_β-H_2 wag + $C_\beta H$ bend
23	1510	14.8	0.75	-0.8	1514	1363	5.6	0.75	-3.5	4.5	0.75	1333	-20.2	$C_\beta H$ bend + C_β-H_2 wag
24	1493	6.6	0.73	-0.8	1493	1344	6.0	0.71	0.3	4.5	0.73			$C_{\alpha'}$-H_2 wag + $C_{\beta'}$-H_2 twist + OC-$C_{\alpha'}$ str
25	1488	1.7	0.75	-4.7	1469	1322	4.8	0.75	-1.3	4.1	0.75	1314	-10.9	$C_\gamma H_2$ wag + $C_\beta H$ bend
26	1449	7.2	0.75	1.7	1436	1292	4.8	0.73	2.9	3.6	0.74	1302	+9.0	$C_\alpha H_2$ wag + $C_\beta H$ bend
27	1430	5.4	0.75	2.0	1411	1270	9.7	0.75	-1.2	8.1	0.75	1265	-14.1	$C_\gamma H_2$ twist + $C_\alpha H_2$ twist + $C_{\alpha'}$-H_2 twist
28	1388	7.0	0.75	-1.5	1369	1232	9.0	0.74	-0.3	7.7	0.74			$C_{\alpha'}$-H_2 twist + $C_\alpha H_2$ twist
29	1385	6.6	0.74	0.2	1360	1224	2.5	0.75	-2.3	2.1	0.75	1223	6.3	$C_\gamma H_2$ twist + $C_{\alpha'}$-H_2 wag + $C_\alpha H_2$ wag + asym C=O bend
30	1352	11.6	0.75	-1.4	1345	1211	12.0	0.75	-0.8	9.8	0.75	1200	10.2	C_β-H_2 twist + $C_\gamma H_2$ wag
31	1277	4.0	0.17	11.9	1261	1135	4.1	0.14	15.2	3.1	0.14	1175	39.1	$C_{\alpha'}$-H_2 rock + C_β-H_2 rock + CH_3 rock
32	1244	3.6	0.73	-0.1	1240	1116	3.5	0.72	0.4	2.8	0.72	1115	-11.5	CH_3 rock + C_α-C_β str + C_β-C_γ str
33	1196	8.4	0.70	1.2	1183	1065	9.1	0.67	-2.2	8.0	0.67	1078	-15.8	C_β-CH_3 str
34	1192	3.1	0.66	-10.8	1162	1046	1.5	0.75	1.1	1.4	0.75	1053	4.7	$C_\alpha H_2$ twist + $C_{\alpha'}$-H_2 twist + $C_\gamma H_2$ twist + $C_\beta H$ bend
35	1149	4.6	0.73	-0.2	1132	1019	6.1	0.74	-0.4	5.1	0.74	1023	-17.1	C_β~C_γ str + C_α~$C_{\beta'}$ str
36	1085	1.4	0.66	-0.8	1061	955	1.5	0.69	-1.5	1.3	0.69			CH_3 rock + $C_\beta H$ bend + C_β-H_2 rock
37	1068	8.7	0.73	2.4	1054	949	8.6	0.73	2.4	7.2	0.74	971	31.8	CH_3 rock + C_β-C_γ str + C_α-C_β-C_γ bend + C_α~$C_{\beta'}$ str
38	1048	8.0	0.67	-2.0	1037	933	8.1	0.65	-2.2	6.5	0.65	945	-17.6	C_α~$C_{\beta'}$ str + C_β-H_2 rock + CH_3 rock + $C_\alpha H_2$ rock
39	974	1.2	0.70	3.5	960	864	0.9	0.45	12.2	0.8	0.43	888	-13.5	C_β~C_γ str + C_α~$C_{\beta'}$ str + $C_\alpha H_2$ rock + $C_\gamma H_2$ rock
40	956	2.8	0.26	1.5	950	855	2.8	0.30	-0.8	2.2	0.29	870	-20.4	$C_\gamma H_2$ rock + C_α~$C_{\beta'}$ str + C_β~C_γ str + $C_\alpha H_2$ rock
41	938	2.7	0.35	4.3	915	824	3.1	0.36	5.2	2.9	0.36	833	11.7	$C_{\alpha'}$-H_2 rock + C-C_α str + $C_\alpha H_2$ rock + CH_3 rock
42	888	1.0	0.23	-9.4	883	795	1.4	0.20	-7.3	1.0	0.24	809	-17.9	C_β-C_γ str + C-C_α str + C-$C_{\alpha'}$ str + C_α-C_β str
43	831	11.4	0.18	0.4	821	739	10.7	0.19	-0.0	9.7	0.18	752	-1.9	C_β-H_2 rock + C-$C_{\alpha'}$ str + C_β-C_γ str + $C_\alpha H_2$ rock
44	693	12.0	0.07	-3.0	692	623	11.8	0.06	-3.4	10.2	0.06	642	-20.5	C=O out-of-plane bend + C_α-C_β str
45	558	2.1	0.38	-10.3	555	500	2.0	0.47	-7.4	1.4	0.40	516	-36.6	C=O in-plane bend + $C_\alpha C_\beta C(H_3)$ bend
46	533	1.7	0.56	9.2	526	473	1.8	0.50	7.3	1.4	0.46	490	37.4	$C_{\alpha'}$-C_β-C_γ bend + $C_{\beta'}$-$C_\gamma C_\beta$ bend
47	472	1.6	0.32	-0.3	464	418	1.7	0.28	-0.1	1.3	0.25	439	0.4	$C_\alpha CC_{\alpha'}$ bend + $C_\gamma C_\beta C(H_3)$ bend + $C_\alpha H_2$ rock
48	438	4.0	0.37	1.4	427	384	3.7	0.38	1.7	3.2	0.37	400	10.8	$C_{\alpha'}$-C_β-C_γ bend + $C_\beta C_\alpha C$ bend + $C_{\beta'}$-$C_{\alpha'}$-C bend
49	419	1.2	0.60	0.5	411	370	1.1	0.67	-0.3	0.8	0.65	386	-13.2	$C_\alpha CC_{\alpha'}$ bend + $C_{\beta'}$-$C_{\alpha'}$-C bend + $C_\beta C_\gamma C_{\beta'}$ bend
50	320	0.2	0.63	-8.5	316	284	0.1	0.63	-8.9	0.1	0.57	300	-21.4	$C(H_3)C_\beta C_\gamma$ bend + $C(H_3)C_\beta C_\alpha$ bend
51	270	0.2	0.72	-10.0	270	243	0.2	0.70	-9.2	0.2	0.71	255	-60.5	$CC_\alpha C_\beta C_\gamma$ torsion + $CC_{\alpha'}$-C_β-C_γ torsion
52	247	0.0	0.72	-3.5	253	228	0.0	0.68	-6.4	0.0	0.67	218		CH_3 torsion
53	140	0.1	0.75	8.8	139	125	0.1	0.75	8.6	0.1	0.75	142	22.3	$CC_\alpha C_\beta C_\gamma$ torsion + $CC_{\alpha'}$-C_β-C_γ torsion
54	103	0.6	0.75	1.7	102	92	0.6	0.74	1.7	0.4	0.75	125		$CC_\alpha C_\beta$ bend + $CC_{\alpha'}$-$C_{\beta'}$ bend + C=O out-of-plane bend

[a] Raman intensity parameters are expressed as $45\bar{\alpha}^2 + 7\beta^2$, in (Å^4/amu). ρ is the depolarization ratio defined as $3\beta^2/(45\bar{\alpha}^2 + 4\beta^2)$. In the 6-31G*/6-31G calculation, normal modes obtained with the 6-31G* basis set and Cartesian polarizability derivative tensors obtained with the 6-31G basis set were used. In addition to the experimental bands listed, weak bands at ~350, 362, 549, 675, 786, 1574, 1611, 1639, 1676, 1713, and 1746 cm^{-1} are apparent in the experimental Raman spectrum. These bands are considered to be due to nonfundamental modes. [b] The assignments were derived from the potential energy distribution and (or) displacements in internal coordinates. These descriptions depend on the choice of internal coordinates used, which is arbitrary. The internal symmetry coordinates employed are as follows: 20 bond stretches, 16 CH_2 bends (four per CH_2 group representing scissors, twist, rock, and wagging motions), 2 methine bends, 2 C–C(H_3) bends, 6 CH_3 bends (representing one symmetric, two asymmetric, two rock, and one torsional motion), 2 C=O bends (one in-plane and one out-of-plane motion), 5 ring bends (one each at C, Cα, Cα′, Cβ′, and Cγ), and a ring torsion.

with the 6-31G and 6-31G* basis sets. The derivatives $\partial\alpha_{\alpha\beta}/\partial X_A$, $\partial G_{\alpha\beta'}/\partial X_A$, and $\partial A_{\alpha\beta\gamma}/\partial X_A$ were obtained numerically by evaluating the tensors $\alpha_{\alpha\beta}$, $G_{\alpha\beta'}$, and $A_{\alpha\beta\gamma}$ at the equilibrium geometries and at geometries displaced by 0.005 Å along each atomic Cartesian coordinate. The need for this numerical method arises from the unavailability at the present time of an analytic procedure for evaluating $\partial G_{\alpha\beta'}/\partial X_A$. The procedure for obtaining $G_{\alpha\beta'}$ is based on the static limit approximation and is due to Amos[35] as implemented in the CADPAC program,[36] which simultaneously evaluates $\alpha_{\alpha\beta}$ and $A_{\alpha\beta\gamma}$. All calculations were done at the fully optimized geometries for the chair conformer with the methyl group in an equatorial position. The vibrational frequencies, normal modes, and Raman intensities were also obtained at the same geometries.

The theoretical Raman and ROA spectra were simulated with Lorentzian band shapes and are compared to the corresponding experimental spectra in Figure 2. The normalized circular intensity differences Δ_z are compared in Table I. The theoretical vibrational frequencies, Raman intensities, and mode descriptions are also summarized in Table I. Three-dimensional displays, similar to those in ref 28, for the 6-31G* modes were generated by adopting the ORTEP program[37] as in the earlier work.[38] These are not presented here but can be obtained from the authors. The theoretical frequencies were multiplied by 0.9 to bring them closer to the experimental values. The frequencies obtained with the 6-31G* basis set and scaled by 0.9 will be used in the discussion, unless specified otherwise.

Results and Discussion

Molecular Structure. The molecular structure of 3-methylcyclohexanone has not been determined experimentally. Previous theoretical studies[22-30,31d-g] on 3-methylcyclohexanone have used

(35) Amos, R. D. *Chem. Phys. Lett.* **1982**, *87*, 23.

(36) Amos, R. D.; Rice, J. E. *CADPAC: Cambridge Analytic Derivative Package*, issue 4.0; Cambridge University: Cambridge, England, 1987.

(37) Johnson, C. K. *ORTEP: A Fortran thermal ellipsoid plot program for crystal structure illustrations*; Oak Ridge National Laboratory: Oak Ridge, TN, 1976.

(38) Polavarapu, P. L.; Pickard, S. T.; Smith, H. E.; Black, T. M.; Rauk, A.; Yang, D. *J. Am. Chem. Soc.* **1991**, *113*, 9747. Hess, B. A., Jr.; Cha, J. K.; Schaad, L. J.; Polavarapu, P. L. *J. Org. Chem.* **1992**, *57*, 6367.

either the idealized[31d] bond lengths and angles or those approximated for related cyclohexanones.[31c,g] With the idealized structural parameters, *ab initio* studies using a minimal basis set predicted[31e] the energy for the chair conformer with the methyl group in an equatorial position to be favorable, over that with the methyl group in an axial position, by ~3 kcal/mol. Experimental circular dichroism[31a,b] and microwave studies[31c] also suggested that the chair form with the methyl group in an equatorial position is preferred and that the populations of other conformers (axial methyl group and twisted ring) are small. On the basis of these previous conclusions we assumed that the chair conformer of 3-methylcyclohexanone with the methyl group in an equatorial position is predominant and optimized the structure of this conformer. The 6-31G* energy of this conformer at the fully optimized geometry is –346.9417 hartrees. The axial C–H bond lengths (C–H_a) are slightly longer than the equatorial C–H bond lengths (C–H_e): C_α–H_a = 1.090, C_α–H_e = 1.083, C_β–H_a = 1.090, $C_{\alpha'}$–H_a = 1.089, $C_{\alpha'}$–H_e = 1.083, $C_{\beta'}$–H_a = 1.088, $C_{\beta'}$–H_e = 1.085, C_γ–H_a = 1.090, C_γ–H_e = 1.086 Å (C, C_α, C_β, C_γ, $C_{\beta'}$, and $C_{\alpha'}$ are, respectively, the carbon atoms at positions 1–6 of the ring). The heavy atom bond lengths are as follows: C–O = 1.19, C–C_α = 1.52, C–C_α = 1.52, C_α–C_β = 1.54, $C_{\alpha'}$–$C_{\beta'}$ = 1.54, C_β–C_γ = 1.53, $C_{\beta'}$–C_γ = 1.53 Å. The heavy atom angles are as follows: OCC_α = 122°, $C_\alpha C C_{\alpha'}$ = 115°, $CC_\alpha C_\beta$ = 112°, $CC_{\alpha'}C_{\beta'}$ = 111°, $C_\alpha C_\beta C_\gamma$ = 110°, $C_{\alpha'}C_{\beta'}C_\gamma$ = 112°, $C_\beta C_\gamma C_{\beta'}$ = 112°, $C_\alpha C_\beta C(H_3)$ = 111°. The HCH angles at α, α', β', and γ positions, respectively, are 108°, 108°, 107°, and 107°. The ring torsional angles are as follows: $\tau(CC_\alpha C_\beta C_\gamma)$ = –52°, $\tau(CC_{\alpha'}C_{\beta'}C_\gamma)$ = 52°, $\tau(OCC_\alpha C_\beta)$ = 131°, $\tau(CC_\alpha C_\beta C(H_3))$ = 177°. Some of these structural parameters are significantly different from the ones previously used; for example, the C=O bond length is 1.19 Å as opposed to the assumed[31c] value of 1.22 Å and the $C_\alpha C C_{\alpha'}$ angle is 115° as opposed to the idealized[31d] value of 120°. A complete list of the structural parameters can be obtained from the authors.

Raman Spectra. The comparison of experimental and theoretical depolarized Raman spectra in Figure 2 indicates that the experimental spectrum is reproduced qualitatively well by both 6-31G and 6-31G* basis set calculations. No major differences are evident among the predictions of 6-31G and 6-31G* basis sets. However, small differences in the relative intensities of the bands in the region around 1350 cm^{-1} are present in these two calculations, where the predicted relative intensities in the 6-31G calculation are closer to the observed ones. The relative Raman intensities obtained in the mixed 6-31G*/6-31G calculation are nearly identical to those in the 6-31G* calculation, indicating that the Cartesian electric dipole polarizability derivative tensors are not influenced significantly by the addition of polarization functions to the 6-31G basis set. This observation is in accord with those reported earlier for other molecules.[6,7,13]

The experimental polarized Raman spectra for different isotopomers of 3-methylcyclohexanone, namely 3-methylcyclohexanone-*3*-d_1, 3-(methyl-d_3)cyclohexanone, 3-methylcyclohexanone-*5,5*-d_2, 3-methylcyclohexanone-*4,4*-d_2, and 3-methylcyclohexanone-*2,2,6,6*-d_4, were reported by Freedman et al.[28] in the ~100–700-cm^{-1} region. The quality of *ab initio* predictions can be tested further by comparing the *ab initio* predictions of Raman spectra for these isotopomers. The simulated spectra obtained with the 6-31G* basis set are shown in Figure 3, and the frequency and intensity data are summarized in Table II. There are 11 modes below 700 cm^{-1} for these molecules. The experimental band positions corresponding to eight of these higher frequency modes, as reported by Freedman et al.,[28] are also summarized in Table II.

The experimental polarized Raman spectrum (not shown here) of 3-methylcyclohexanone in the 100–700-cm^{-1} region is similar to the corresponding depolarized Raman spectrum shown in Figures 1 and 2, except that the band at 642 cm^{-1} being strongly polarized has significantly larger intensity in the former. The

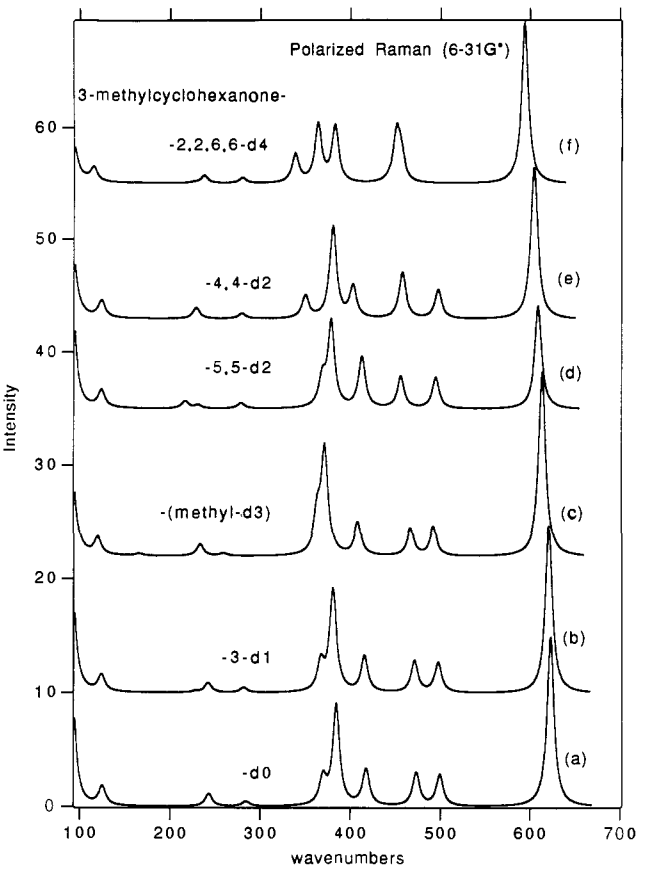

Figure 3. *Ab initio* theoretical polarized Raman spectra obtained with the 6-31G* basis set for (a) 3-methylcyclohexanone, (b) 3-methylcyclohexanone-*3*-d_1, (c) 3-(methyl-d_3)cyclohexanone, (d) 3-methylcyclohexanone-*5,5*-d_2, (e) 3-methylcyclohexanone-*4,4*-d_2, and (f) 3-methylcyclohexanone-*2,2,6,6*-d_4. All spectra are on the same relative intensity scale but are shifted from each other for clarity. The 6-31G* frequencies were multiplied by 0.9 to bring them closer to the experimental values, and the spectra were simulated with Lorentzian band shapes and a 5-cm^{-1} half width.

corresponding 6-31G* theoretical mode with a scaled frequency of 632 cm^{-1} is also predicted to be strongly polarized with a depolarization ratio of only 0.06. This mode has a major contribution from the out-of-plane C=O bending motion. The internal coordinate coupling associated with this mode varies in the isotopomers of 3-methylcyclohexanone, and this variation causes the intensity and frequency associated with this mode to change. It is of interest to note that the predicted frequency of this mode decreases in the order of isotopomers shown in Figure 3, and an identical order of frequency shifts was observed[28] for the corresponding experimental bands (see Table II). The intensity of this mode is not significantly influenced in the -*3*-d_1 and -(methyl-d_3) isotopomers but decreases by nearly half in the -*5,5*-d_2 isotopomer and then increases from that value by ~1.5 in the -*4,4*-d_2 and -*2,2,6,6*-d_4 isotopomers. Identical relative trends were found[28] for the corresponding experimental Raman bands.

In the 300–500-cm^{-1} region, the spectral pattern seen for the parent molecule is retained, with minor frequency shifts, for the -*3*-d_1 and -(methyl-d_3) isotopomers. One point of interest here is that the two modes with scaled frequencies of 370 and 384 cm^{-1} for the parent molecule give rise to resolved bands in the simulated spectrum, but for the -(methyl-d_3) isotopomer they are predicted to be closer in frequency, at 364 and 372 cm^{-1}, resulting in poorly resolved bands in the simulated spectrum. This predicted pattern is in agreement with that observed in the experimental spectra.[28] The spectral pattern in this region is predicted to be significantly different for the -*4,4*-d_2 and *2,2,6,6*-d_4 isotopomers, and the predicted patterns for these molecules are nearly identical to those seen in the experimental spectra.[28] One minor discrepancy

Table II. Vibrational Frequencies and Raman Intensities for Isotopomers of 3-Methylcyclohexanone[a]

-d_0					-3-d_1					methyl-d_3				
$\bar{\nu}$ (cm^{-1})			Raman		$\bar{\nu}$ (cm^{-1})			Raman		$\bar{\nu}$ (cm^{-1})			Raman	
6-31G*	scaled	expt	$45\bar{\alpha}^2+7\beta^2$	ρ	6-31G*	scaled	expt	$45\bar{\alpha}^2+7\beta^2$	ρ	6-31G*	scaled	expt	$45\bar{\alpha}^2+7\beta^2$	ρ
692	623	642	10.0	0.06	690	621	639	10.0	0.06	682	614	635	10.9	0.07
555	500	514	1.4	0.40	553	498	511	1.3	0.46	547	492	506	1.3	0.59
526	473	490	1.4	0.40	524	472	488	1.3	0.45	519	467	485	1.1	0.50
464	418	439	1.3	0.25	462	416	437	1.3	0.28	454	409	429	1.1	0.50
427	384	398	3.2	0.37	423	381	395	3.2	0.36	413	372	383	3.2	0.38
411	370	388	0.8	0.65	408	367	385	0.8	0.71	404	364	383	1.1	0.27
316	284	299	0.1	0.57	313	282	295	0.1	0.57	288	259	270	0.0	0.47
270	243	259	0.2	0.71	269	242	258	0.2	0.71	259	233	248	0.2	0.75
253	228		0.0	0.67	253	228		0.0	0.66	184	166		0.0	0.74
139	125		0.1	0.75	138	124		0.1	0.75	133	120		0.1	0.74
102	92		0.4	0.75	101	91		0.4	0.75	100	90		0.4	0.75
-5,5-d_2					-4,4-d_2					-2,2,6,6-d_4				
$\bar{\nu}$ (cm^{-1})			Raman		$\bar{\nu}$ (cm^{-1})			Raman		$\bar{\nu}$ (cm^{-1})			Raman	
6-31G*	scaled	expt	$45\bar{\alpha}^2+7\beta^2$	ρ	6-31G*	scaled	expt	$45\bar{\alpha}^2+7\beta^2$	ρ	6-31G*	scaled	expt	$45\bar{\alpha}^2+7\beta^2$	ρ
677	609	625	6.1	0.08	672	605	620	8.9	0.06	660	594	613	9.2	0.08
550	495	511	1.4	0.38	553	498	510	1.3	0.40	507	456	469	1.0	0.39
507	456	476	1.3	0.45	509	458	472	1.9	0.30	501	451	469	2.0	0.37
459	413	435	1.8	0.21	448	403	421	1.1	0.66	425	383	399	1.8	0.15
421	379	395	2.7	0.43	423	381	393	2.9	0.40	404	364	376	1.8	0.68
410	369	388	0.8	0.65	389	350	364	0.6	0.33	376	338	353	0.8	0.75
310	279	295	0.1	0.66	311	280	294	0.1	0.64	311	280	295	0.1	0.56
257	231	230	0.1	0.74	255	230	242	0.1	0.67	264	238	253	0.1	0.71
241	217		0.1	0.67	253	228		0.0	0.65	252	227		0.0	0.64
138	124		0.1	0.75	138	124		0.1	0.75	128	115		0.1	0.74
101	91		0.4	0.75	99	89		0.4	0.75	97	87		0.4	0.75

[a] Scaled frequencies were obtained by multiplying the 6-31G* frequencies by 0.9. Raman intensity oparameters ($45\bar{\alpha}^2+7\beta^2$) and the depolarization ratio (ρ) were obtained with the 6-31G* basis set. The experimental frequencies are from ref 28.

is that the two modes of the -2,2,6,6-d_4 isotopomer with scaled frequencies of 376 and 399 cm^{-1} are predicted to have equal intensities, whereas the corresponding experimental bands at 364 and 383 cm^{-1} have unequal intensities with the former slightly less intense than the latter.

The two modes in the 200–300-cm^{-1} region are predicted to be weak for all of the molecules considered here. The variations in frequencies and intensities of these modes among the isotopomers are similar to the corresponding variations seen in the experimental spectra.

Raman Optical Activity. The depolarized ROA spectrum of (*R*)-(+)-3-methylcyclohexanone presented here reproduces all of the major features reported several years ago using an older generation ROA instrument.[39] A comparison of the experimental and theoretical ROA spectra (Figure 2) indicates that for a large number of bands the ROA signs observed for (+)-3-methylcyclohexanone and those predicted for (*R*)-3-methylcyclohexanone are in agreement. As in the Raman spectra, there are no major differences among the ROA predictions obtained in the 6-31G and 6-31G*/6-31G calculations.

The correlation between the theoretical modes and the experimental bands, presented in Table I, is obtained from a consideration of the relative Raman intensities as well as the ROA signs. Due to the presence of a large number of vibrations for this molecule in the 100–1800-cm^{-1} region, and since all of the ROA features associated with these vibrations may not be of general interest, the discussion will be restricted to those ROA features that have attracted attention in the literature. For the remaining ROA and Raman bands the reader can find the appropriate information in Table I.

Couplet in the 130–260-cm^{-1} Region. The positive–negative ROA couplet observed in this region was thought to have[26] a major contribution from the methyl torsion vibration. This was partly based on the assertion that the methyl torsion in methylcyclohexane occurs at 237 cm^{-1} and on the predictions of the inertial model.[40] The frequency range associated with the methyl torsion mode is supported by the present *ab initio* calculations. The scaled 6-31G* frequency for this mode is 228 cm^{-1}. The present calculations indicate that the Raman intensity associated with the methyl torsion mode is not significant enough to be observed in the Raman spectrum. The weak Raman band present in the experimental spectrum at 218 cm^{-1} probably corresponds to this mode. Nevertheless, a moderate-size negative Δ_z value is predicted in the present calculations for this mode, and therefore it is possible to assume that the negative ROA in the experimental spectrum sloping toward the 255-cm^{-1} band might be associated with the methyl torsion Raman band.

It is clear that the methyl torsion vibration has very weak Raman and ROA intensities. Therefore it is unlikely that the methyl torsion mode will serve as a useful marker for determining the absolute configuration in general, but for small molecules such as *trans*-2,3-dimethyloxirane and *trans*-2,3-dimethylthiirane, the methyl torsion ROA was indeed found to be useful.[11,12] The present calculations suggest that, in the immediate vicinity of the methyl torsion band, the observed positive ROA at 142 cm^{-1} originates from a ring mode predicted to appear at an unscaled *ab initio* frequency of 139 cm^{-1} and the negative observed ROA at 255 cm^{-1} originates from another ring mode predicted to appear at an unscaled *ab initio* frequency of 270 cm^{-1}. These two modes have larger contributions from the torsional motions around the C_α–C_β and $C_{\alpha'}$–$C_{\beta'}$ bonds. The normal mode for the unscaled 139-cm^{-1} frequency has a significant contribution from C–CH_3 stretching but no significant CCH_3 bending motion, unlike the mode description derived from the empirical force field calculation.[28] It is of interest to note that in the experimental spectrum a neighboring negative ROA band at 300 cm^{-1} is predicted to originate from the bending of the methyl carbon atom (relative to the ring carbon atoms) and this mode has observable Raman intensity. Therefore, the H_3C–C–C bending motion may serve

(39) Barron, L. D. *J. Chem. Soc., Perkin Trans. 2* **1977**, 1074.

(40) Barron, L. D.; Buckingham, A. D. *J. Am. Chem. Soc.* **1979**, *101*, 1979.

as a better ROA signature of the methyl group at the chiral center than the methyl torsion mode.

Couplet in the 380–410-cm^{-1} Region. The observed negative–positive couplet, from the low-frequency side, is associated with the broader Raman band with a resolved low-frequency shoulder. The present calculations indicate that the two modes at 370 and 384 cm^{-1} are responsible for the observed Raman band and the associated ROA couplet. The negative portion of the couplet is not seen in the simulated spectrum, because of small magnitude, but the 370-cm^{-1} mode is indeed predicted to have negative ROA (see Table I). Therefore the current predictions are in reasonable agreement with the observed Raman and ROA features, and the associated mode descriptions might be considered reliable. The 384-cm^{-1} mode is essentially a ring-bending mode, and that at 370 cm^{-1} has significant contributions from the $C_\alpha CC_{\alpha'}$ bending motion as well as ring-bending motions. Earlier analyses[23,28] employing empirical force fields also attributed these two modes to ring-bending motions, but the internal coordinate couplings obtained in those calculations appear to be different from the ones obtained in the present *ab initio* calculations (as deduced from the comparison of the present normal mode displays with those in ref 28).

Couplet in the 480–520-cm^{-1} Region. The observed positive–negative couplet, from the low-frequency side, is correctly reproduced in the theoretical spectrum, as are the corresponding relative Raman intensities. The theoretical modes are predicted to occur at 473 and 500 cm^{-1}, corresponding to the observed band positions of 490 and 516 cm^{-1}, respectively. The former mode is due to a ring-bending mode and the latter due to the in-plane C=O bending motion that is coupled with the bending motion of the methyl carbon atom (relative to the ring). The mode description for the 516-cm^{-1} band is quite similar to that suggested by Barron and Clark.[26] However, unlike the earlier prediction, there is no significant in-plane C=O bending contribution to the 490-cm^{-1} band. The prediction by Freedman and co-workers[28] that the observed bands at 490 and 516 cm^{-1} are due to in- and out-of-phase combinations of in-plane C=O bending with ring deformation is not supported by the present results. In this context it is of interest to note that the weak Raman and negative ROA sign characteristics predicted for the theoretical out-of-plane C=O bending mode at 623 cm^{-1} correspond very nicely to the observed weak Raman and negative ROA observed at 642 cm^{-1}.

Couplet in the 930–980-cm^{-1} Region. The bisignate couplet observed in this region consists of a negative band at 945 cm^{-1} and a strong positive band at 971 cm^{-1}. The ROA signs seen in the simulated spectrum agree with these signs. However, the relative theoretical ROA intensities of these two components are not in complete agreement with the experimental observation. The simulated spectrum shows nearly equal intensities for the bisignate couplet, whereas in the experimental spectrum the negative is about half the intensity associated with the positive component. There are three modes at 933, 949, and 955 cm^{-1} which are apparently responsible for the observed couplet. Two of these, at 949 and 955 cm^{-1}, are due to the two methyl rocking modes with oppositely signed ROA of unequal intensity, and their close proximity results in significant cancellation; the positive ROA comes from what is left after cancellation. The negative ROA originates from the 933-cm^{-1} mode that is due to a ring stretch coupled to the methylene and methyl group bending motions. These mode predictions are different from the earlier hypotheses which associated the bisignate couplet to the two methyl rocking modes. Although the present calculations predict these two modes to have opposite ROA signs, the facts that one of them has weak Raman and ROA and that they overlap significantly make it difficult to suggest that ROA associated with these two modes is resolved in the experimental spectrum.

The interpretation offered by Zimba et al.[29] for the ROA couplet under discussion, however, raises some further questions. They reported three ROA bands at 969, 960, and 946 cm^{-1} with positive, negative, and negative ROA signs, respectively. The presence of three bands here is supported by the present calculations as well as by the presence of three bands in this region of the infrared absorption and higher resolution Raman spectra. Two of the bands reported by Zimba et al. at 969 and 946 cm^{-1} probably correspond to the present experimental bands at 971 and 945 cm^{-1}. The negative ROA band at 960 cm^{-1} does not have a counterpart in the present experimental spectrum and is most likely an ROA artifact. However, if their observation is correct, then the predicted order of the two methyl rocking modes in the present calculations has to be interchanged. The suggestion that their 946-cm^{-1} band originates from the C–CH_3 stretch is not supported by the present results.

Other Couplets in the 1000–1500-cm^{-1} Region. There are four closely spaced couplets clearly resolved in the experimental spectrum in this region. The origin of these couplets can be deduced from the corresponding theoretical predictions. The negative–positive–negative triplet in the 1020–1090-cm^{-1} region appears to originate from the ring C–C stretches, CH_2 twist, and C–CH_3 stretching vibrations. Another positive–negative couplet in the 1200–1280-cm^{-1} region originates from different CH_2 twisting vibrations. The third positive–negative couplet in the 1300–1350-cm^{-1} region originates from the CH_2 wagging motions and a methine bending vibration coupled to CH_2 wagging. The couplet associated with the 1423- and 1459-cm^{-1} Raman bands cannot be easily assigned to a specific pair of modes. The calculated frequencies indicate that there are several modes that contribute to the observed bands in this region.

The 1000–1500-cm^{-1} region has several vibrational modes with significant overlap. Such crowding in the spectrum makes it difficult to draw useful correlations with the molecular structure because slight perturbations can lead to rearrangements in the order of the predicted bands and therefore uncertainties in interpretations. These uncertainties are probably responsible for the poor correlation between the predicted and observed ROA features in this region. One way to improve the situation here is to adjust the force constants by verifying and fitting the calculated vibrational frequencies and intensities to the corresponding experimental data for isotopic molecules, but the experimental data for isotopic molecules in this region are not available.

Couplet at ~1700 cm^{-1}. Only one C=O stretching band is expected for methylcyclohexanone if this molecule has just one predominant conformer. The strong Raman band at 1710 cm^{-1} with a weak shoulder at 1713 cm^{-1} and the presence of a bisignate couplet (or possibly a triplet) associated with these bands suggest that either methylcyclohexanone exists as two or more different conformers or the weak band at 1713 cm^{-1} is due to one or more nonfundamental vibrations. Since the literature data point to the predominance of a single conformation, and the experimental Raman spectrum also has weak bands in the 1600–1680-cm^{-1} region which cannot be associated with any fundamental modes, it is very likely that the weak Raman band at 1713 cm^{-1} and the associated weak ROA features are due to nonfundamental vibrations. The possibility for a ROA artifact here can be verified by measuring the ROA spectrum for the (–)-enantiomer, but this enantiomer is currently not available. The possibility that the ROA structure in this region is associated with Fermi resonance involving the C=O stretch and one or more overtones should also be considered since Escribano[41] has shown theoretically that the interaction between a fundamental and an overtone can take the form of a characteristic bisignate couplet.

CH_3 Group Bending Vibrations. In the early stages of the development of VOA, it was thought[42,43] that the two asymmetric

(41) Escribano, J. R. Doctoral Thesis, The University, Glasgow, 1985.
(42) Barron, L. D. *Nature* **1975**, *255*, 458.
(43) Nafie, L. A.; Polavarapu, P. L.; Diem, M. *J. Chem. Phys.* **1980**, *73*, 3530.

bending motions of the methyl group might serve as chiral probes, since these two modes are expected to give a bisignate couplet that could reveal the absolute configuration at the chiral center. However, these two modes in most cases have nearly the same vibrational frequency, which is also the case here for methylcyclohexanone (Table I), resulting in mutual cancellation of their ROA. The symmetric bending vibration of the methyl group usually has weak Raman and ROA intensities in the depolarized spectra and in most cases is overlapped by the other C–H bending vibrations. Noting that the methyl torsion vibration also has very weak Raman and ROA and the two methyl rocking modes have mutually cancelling unresolved ROA (*vide supra*), the methyl group vibrations are unlikely to be useful as probes of absolute configuration in the solution phase. This situation can be different if ROA studies are carried out on matrix isolated molecules, where closely spaced vibrations might be resolvable.

Conclusions

The predicted Raman and ROA spectra are found to be in reasonable agreement with the experimental observations. In particular, the overall ROA sign pattern observed for (+)-3-methylcyclohexanone is well reproduced by the calculations for (*R*)-3-methylcyclohexanone. Since the (+)-enantiomer is indeed known to have the (*R*)-configuration, and the conformation used here is known to be the dominant conformer, this observation renders support for the *ab initio* theoretical model employed and suggests that the absolute configurations can be predicted confidently with ROA. The vibrational assignments resulting from the current *ab initio* study point to the difficulties in placing reliance on those deduced from the empirical vibrational analysis. In a medium-size molecule such as methylcyclohexanone, the numerous vibrations that overlap in the limited vibrational frequency region make it generally difficult to confidently hypothesize (on the basis of group assignments and intuition) the vibrational origin of the observed bands. It is therefore necessary to exercise caution in deducing the conformation or absolute configuration from the hypothesized vibrational assignments. In particular it is often tempting to associate a bisignate couplet with orthogonal modes such as in-phase and out-of-phase combinations of vibrational coordinates because such modes can be predicted with empirical models to have oppositely signed ROA. However, one should seriously consider the frequency separation between such modes, the possibility that one of the modes may not have significant intensity due to coupling with other internal coordinates, and that a different vibrational band can appear in the immediate vicinity. These factors are difficult to know beforehand, and interpretations of measured VOA spectra therefore demand reliable VOA calculations. The present *ab initio* ROA calculation should not be taken as the final word, however, due to the uncertainties in the *ab initio* force constants expected at the level of theory employed and also due to the uncertainties in correlating the predicted and observed bands when the bands are closely spaced. Nevertheless, the agreement between the experimental and predicted Raman spectra and between the experimental and predicted ROA sign patterns provides some confidence in the interpretations resulting from the present calculations.

Acknowledgment. Grants from the National Science Foundation (CHE8808 18), the Science and Engineering Research Council, the Wolfson Foundation, and the Deutsche Forschungsgemeinschaft (Habilitandenstipendium II C1-He 1588/3-1) are gratefully acknowledged.